Nuclear Instruments and Methods in Physics Research A 621 (2010) 310–315

Contents lists available at ScienceDirect

Nuclear Instruments and Methods in Physics Research A

journal homepage: www.elsevier.com/locate/nima

Development of a position decoder circuit for PET consisting of GAPD arrays

Jin Ho Jung [a,b], Yong Choi [a,b,*], Key Jo Hong [a,b], Wei Hu [a,b], Ji Hoon Kang [a,b], Byung Jun Min [a,b], Seung Han Shin [a,b], Hyun Keong Lim [a,b], Yoon Suk Huh [a,b], Eun-Jeong Kim [c]

[a] Department of Electronic Engineering, Sogang University, 1 Sinsu-dong, Mapo-gu. Seoul 121-742, Korea
[b] Department of Nuclear Medicine, Samsung Medical Center, Sungkyunkwan University School of Medicine, 50 Ilwon-Dong, Kangnam-Ku, Seoul 135-710, Korea
[c] Mesamedical Co. Ltd., Seoul 137-130, Korea

ARTICLE INFO

Article history:
Received 1 December 2009
Received in revised form
5 January 2010
Accepted 7 April 2010
Available online 13 April 2010

Keywords:
Channel reduction technique
Position decoder circuit
Digital address
Analog pulse

ABSTRACT

Use of channel reduction techniques that reduce the number of signals transmitted to a data acquisition (DAQ) module can lead to more efficient use of the DAQ module for PET with numerous readout channels. The purpose of this study was to develop a position decoder circuit (PDC) with a capacity to output the digital address and analog pulse of one interacted channel from numerous PET outputs. A PDC capable of reducing the number of readout channels by a factor of 32 was designed and fabricated. PET detector modules consisting of an LYSO scintillator, a 4×4 array Geiger-mode avalanche photodiode (GAPD), and a 16-channel preamplifier were also constructed to evaluate the performance of the PDC developed for this study. The output signal from the PET detector module was transmitted to the DAQ module after a 45 ns delay by the PDC. Using the gain correction circuit implemented in the PDC, gain uniformity for all channels of the PET detector module was improved by 80%. Energy resolution in the PET detector was 20.4% with the PDC and 20.8% without the PDC. Timing resolution was 2.2 ns with the PDC and 1.5 ns without the PDC. A hot-rod phantom image was successfully acquired using proof-of-principle PET with the PDC developed for this study. Experimental results indicate that the PDC developed for this study is not only useful for the reduction of the readout channel number from the PET detector module consisting of GAPD arrays, but also for PET signal processing and PET imaging.

1. Introduction

The Geiger-mode avalanche photodiode (GAPD), a solid-state photo-sensor consisting of a matrix of independent micro avalanche photodiodes, operates in limited Geiger mode. The GAPD produces a high gain ($\sim 10^6$) signal with high signal-to-noise ratio while it is operated at low voltage (50–70 V), and also offers a fast response with a rise time of less than l ns. Due to the advantages mentioned above, several groups have recently reported on the performance of the GAPD, and have demonstrated its usefulness for PET applications [1–4].

A brain PET system consisting of GAPD arrays is under development in our group. The PET is composed of 72 detector modules arranged in a ring of 330 mm diameter. Each PET detector module consists of a cerium-doped lutetium yttrium orthosilicate (LYSO) scintillator coupled to a 4×4 array GAPD and a 16-channel preamplifier. This configuration of the detector module leads to 1152 channel outputs from the entire PET system. Because only one coincidence event occurs at a time, most of these outputs contain useless information, such as electrical noise or low energy scattered events. Therefore, individual channel readout is unnecessary, and construction of a cost effective readout system using a reduced data acquisition (DAQ) module after selection of only the useful signals is possible.

Among the various methods proposed for reduction of the number of readout channels, the approach using a resistive charge divider is widely used because it is simple, inexpensive, and easy to apply [5–8]. However, this method has several disadvantages, including increased noise due to addition of a number of input channels connected to the resistive charge divider and decreased positioning linearity at the edge of the field of view.

To overcome the disadvantage of the resistive charge divider, several advanced channel reduction methods have been developed. One of these methods involvers use of a multiplexer circuit, which reduces channel numbers by switching the interacted channel with coincidence events among numerous input channels with a voltage level above low-level discrimination (LLD) threshold [9–11]. Use of comparator is another method for identification of the interacted channel [12]. In this way, one or two channels are identified by comparison of all input signals to LLD threshold. Identification of the interacted channel by LLD has some limitations in its application to PET electronics. If signal to noise

* Corresponding author. Tel.: +82 2 705 8910; fax: +82 2 706 4216.
E-mail address: ychoi@skku.edu (Y. Choi).

0168-9002/$ - see front matter © 2010 Elsevier B.V. All rights reserved.
doi:10.1016/j.nima.2010.04.028

ratio of the developed PET system is bad, the number of channels above threshold can frequently be zero or more than one channel. Therefore, improvement of the multiplexing method is a necessity.

The purpose of this study was to develop a high ratio channel reduction method that employs the fastest signal identification method, in addition to application of the LLD for identification of the interacted channel. A position decoder circuit (PDC) with a capacity to output the digital address and analog pulse of one interacted channel from numerous outputs of the GAPD PET detector, was designed and constructed. Signal processing time of the PDC was measured. To compare the performance of the PET detector with and without the PDC, gain uniformity and energy and timing resolutions were also measured. A hot-rod phantom image was acquired to validate feasibility of the PDC for PET imaging.

2. Materials and methods

2.1. Design of the position decoder circuit

A position decoder circuit (PDC) capable of reducing 32 GAPD PET detector outputs to one channel address and one pulse signal was designed. The primary function of the PDC included offset voltage level control, gain adjust, signal delay, signal switching, energy discrimination, and digital signal processing.

In order to shift DC offset of the output signal of the PET detector to ground level, the offset level translation circuit was designed using the amplifier, which is stable at a gain of 1. The offset level was adjusted by changing the value of the variable resistor connected to output of the device supplying the reference voltage. An analog circuit capable of adjusting the gain of the PET detector output was also designed. By adjusting the value of a variable resistor connected in a series to the output of the offset level translation circuit, the gain was varied in the range from 1 to 2. Fig. 1 shows the analog circuit capable of adjusting DC offset level and gain of PET detector output signals.

As illustrated in Fig. 2, a signal delay circuit with a constant group delay of 35 ns across the specified frequency band from 10 to 15 MHz was designed using a high speed (>300 MHz) operational amplifier (op-amp), which is available in a tiny surface mount device (SMD) package that features low cost and low power consumption.

Signal switching and energy discrimination circuits were designed using a device that was carefully chosen to reduce the total propagation delay of the PDC. The device, which has a low on-state resistance of 12 Ω and fast turn on/off time of 5.7/3.8 ns, was chosen as an analog switch. A comparator offering a short propagation delay of 3.5 ns was selected. Fig. 3 shows signal switching and energy discrimination circuits.

Field-programmable gate array (FPGA), which provides 2500 usable gates with pin-to-pin delays as fast as 6 ns and counter speeds of up to 147 MHz, was used to program a digital signal processing algorithm with the capacity to identify the fastest signal among output signals of the comparators and to reduce propagation delay of the PDC.

Fig. 4 illustrates the configuration of the PDC processing the above-mentioned functions. Output signals of the GAPD PET detector were fed into an offset level translation circuit for adjustment of offset voltage level and then sent to the gain adjust circuit for achievement of gain homogeneity for all channels of the detector. Amplified signals were split into two signals. One signal was delayed for 35 ns by the signal delay circuit until the analog switch was turned on. When the switch was turned on, the delayed signal was transferred to the external data acquisition (DAQ) module. The other signal was fed into the comparator, which was used to generate a trigger signal if the signal voltage was above the low level discriminator threshold. Threshold voltage was adjusted by 10 bit precision digital to analog

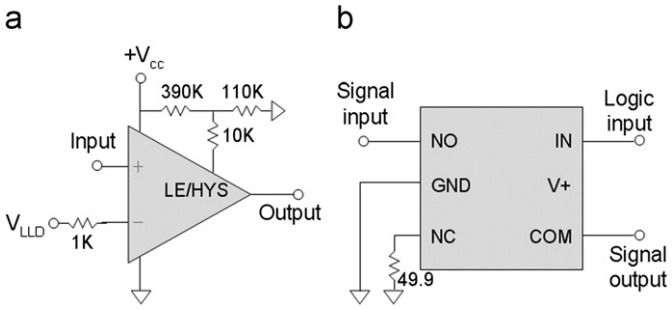

Fig. 3. Signal switch (a) and energy discrimination (b) circuits.

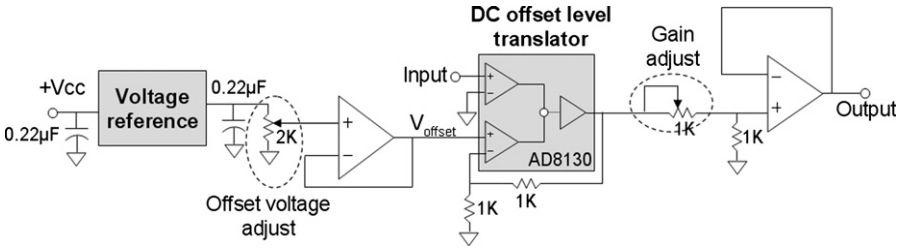

Fig. 1. Analog circuit capable of adjusting DC offset level and gain of PET detector output signals.

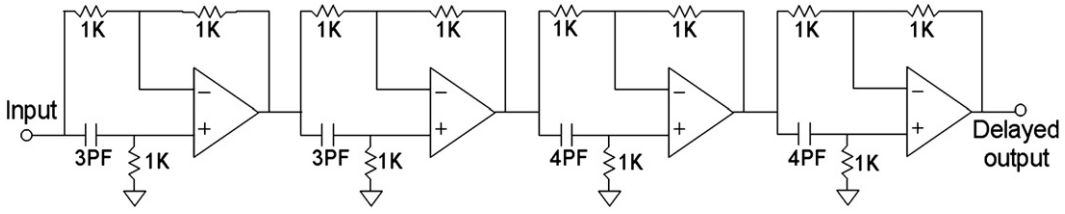

Fig. 2. Signal delay circuit with a propagation delay of 35 ns across a frequency range from 10 to 15 MHz.

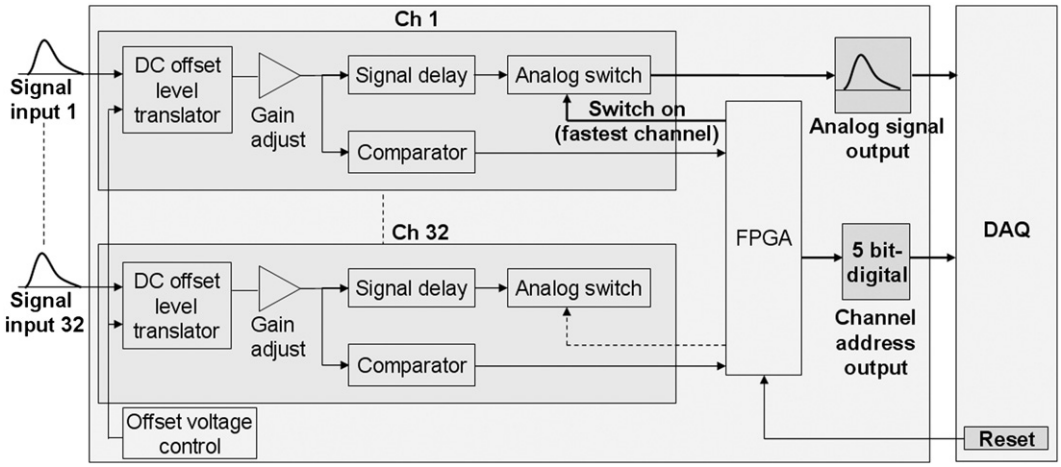

Fig. 4. Schematic diagram representing the configuration of the position decoder circuit.

converter. Trigger signals from several comparators were sent to the FPGA. If the time difference between two trigger signals was larger than 100 ps, the fastest signal was identified by the FPGA and the channel address corresponding to the fastest signal was fed into the DAQ module. The FPGA was reset using the trigger signal transmitted from the DAQ module. On the other hand, if the time difference was smaller than 100 ps, the FPGA was self-reset. The high-level voltage signal (3.5 V) for turning on the analog switch was also generated by the FPGA, and was then sent to the analog switch.

2.2. Performance evaluation of the position decoder circuit

2.2.1. Experimental setup

Two PET detector modules were constructed to evaluate the performance of the PDC. Each detector module consisted of an LYSO (Sinoceramics, Shanghai, China) scintillator block coupled to a 4×4 array GAPD (SensL, Cork, Ireland) and a 16-channel preamplifier. The scintillator block was composed of a 4×4 matrix of $3\,\text{mm}\times3\,\text{mm}\times20\,\text{mm}$ crystals. Individual crystal elements were mechanically polished on all sides and optically isolated with a 0.3 mm white epoxy resin. Each pixel of the GAPD array had a $2.85\,\text{mm}\times2.85\,\text{mm}$ sensitive area and a 3.3 mm pitch. The scintillator was directly coupled to the GAPD without optical-coupling material. Each PET detector module was encapsulated from light. The gain of the preamplifier was 1000, and amplitude, rising time and falling time of the amplified signal generated by 511 keV gamma-ray were 250 mV, 30 ns, and 170 ns, respectively.

Two PDCs were also fabricated; each circuit was capable of identifying one interacted channel from the 32 outputs of the two PET detector modules. Channel address and pulse signal of one interacted channel were sent to the data acquisition (DAQ) module.

The DAQ module with free-running ADC and FPGA containing programmable logic was used to process output signals from the PET detector modules with and without PDC. Energy and starting time of a digitized pulse signal were calculated and stored. Additionally, a trigger signal was generated to reset the FPGA of the PDC; that signal was sent to the PDC after 320 ns, which was required for digitization of the analog signal transmitted from the PDC.

2.2.2. Signal processing time of position decoder circuit

A Gaussian pulse with a 200 ns width and 1 V amplitude was generated using a pulse generator, and the signal was sent to the developed PDC. Propagation delay between input and output was measured to evaluate signal processing time of the PDC.

2.2.3. Gain uniformity and energy resolution measured with and without position decoder circuit

Two PET detector modules were positioned parallel to one another, and a Na-22 point source with an activity of 220 kBq was placed at a distance of 50 mm from the surface of the module. Thirty-two outputs from both detector modules were sent to one PDC. Individual energy spectra for all output channels of the detector modules with and without the PDC were acquired for 10 min and 1 min for acquisition of a similar total count in both cases, respectively. Photopeak positions of the spectra were taken to evaluate the effect of gain correction by the gain adjust circuit implemented in the PDC. Energy resolutions were also evaluated.

2.2.4. Timing resolution measured with and without position decoder circuit

Two PET detector modules were located at opposite sides of each other and separated by 10 mm. A 220 kBq Na-22 point source was placed at the center between them. Output signals from each detector module were independently processed using each PDC. Single events using each detector module with and without the PDC were acquired for 30 min and 3 min for acquisition of a similar total count in both cases, respectively. Coincidence events were then calculated using a 10 ns time window and an energy window of 350–650 keV, and coincidence timing spectra were acquired. Timing resolutions were measured.

2.3. Imaging performance of proof-of-principle PET with PDC

As shown in Fig. 5, a proof-of-principle PET system consisting of 8 pairs of the PET modules covering an arc of 80° with a diameter of 330 mm was constructed. A hot-rod phantom filled with 185 MBq F-18 was located at the center of the field of view. The phantom consisted of 21 rods with various diameters of 5, 6, 7, 8, and 9 mm arranged in five sectors. Phantom data was acquired for 5 s per projection to evaluate the imaging capability of proof-of-principle PET with the PDC. Projection data were also collected at 3° increments over 180° in step-and-shoot mode. The phantom image was reconstructed using a 2D ordered subsets expectation maximization algorithm with 10 iterations and 2 subsets.

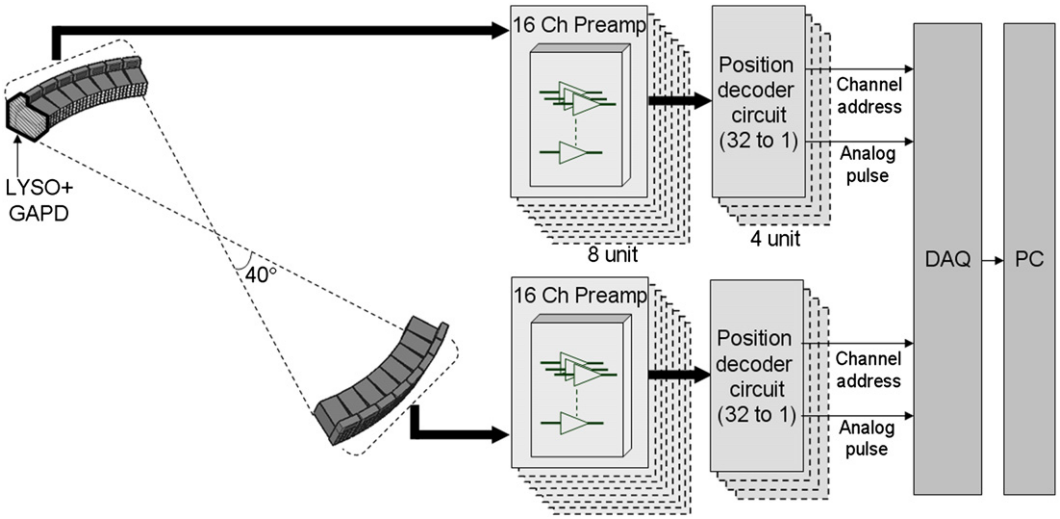

Fig. 5. Schematic diagram of the proof-of-principle PET system consisting of 8 pairs of PET detector modules and signal processing circuits.

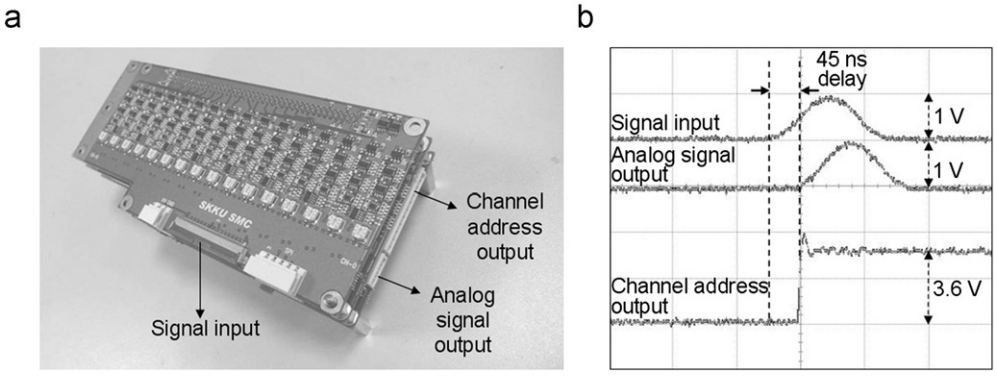

Fig. 6. Photograph of the fabricated position decoder circuit board (a), and propagation delay between input and output signals measured with an oscilloscope (b).

3. Results

3.1. Signal processing time of the position decoder circuit

Fig. 6(a) and (b) shows the fabricated PDC board and the typical timing of its input and output signals, which were measured using an oscilloscope, respectively. Compared with input signal, analog and channel address output signals were delayed about 45 ns. No meaningful distortion of analog output signal was observed.

3.2. Gain uniformity and energy resolution measured with and without position decoder circuit

Thirty-two energy spectra were acquired using two PET detector modules with and without the PDC, and photopeak positions in the energy spectra were measured. Fig. 7(a) shows the energy spectra of one channel among 32 energy spectra. Average energy resolution in detector modules was $20.4 \pm 3\%$ with the PDC and $20.8 \pm 3.1\%$ without the PDC. As illustrated in Fig. 7(b), the ratio of highest and lowest photopeak positions was improved from 1.8 to 1.0 after gain correction using the gain adjust circuit.

3.3. Timing resolution measured with and without the position decoder circuit

As shown in Fig. 8, coincidence timing spectra were measured using a pair of PET detector modules with and without the PDC. Timing resolution in detector modules was 2.2 ns with the PDC and 1.5 ns without the PDC.

3.4. Imaging performance of proof-of-principle PET with PDC

A tomographic image of the hot-rod phantom was acquired using the proof-of-principle PET with the PDC. As illustrated in Fig. 9, the activity distribution pattern of the hot-rod phantom was well imaged without distortion, and all rods were also clearly resolved.

4. Discussion

Use of channel reduction techniques that reduce the number of signals transmitted to the data acquisition (DAQ) module can lead to more efficient use of the DAQ module for PET with numerous readout channels. In this study, a position decoder circuit (PDC), which outputs digital address and analog pulse of one

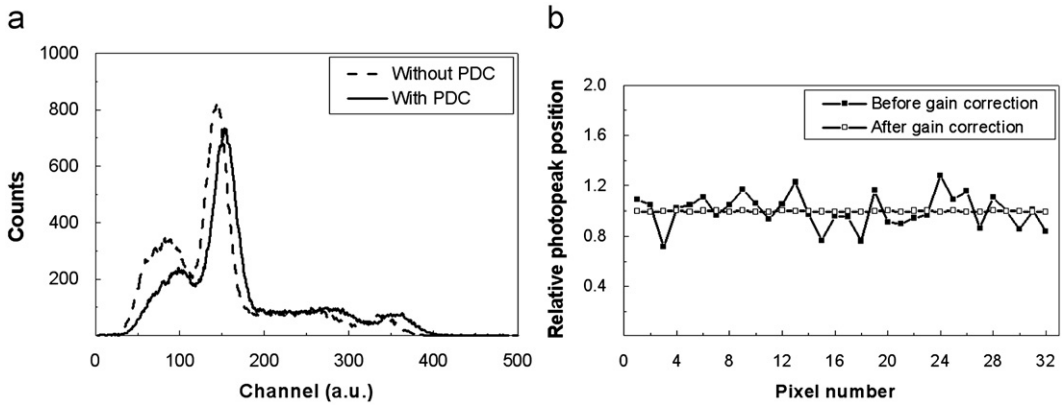

Fig. 7. Energy spectra (a) acquired with and without the position decoder circuit. Relative photopeak positions (b) before and after gain correction.

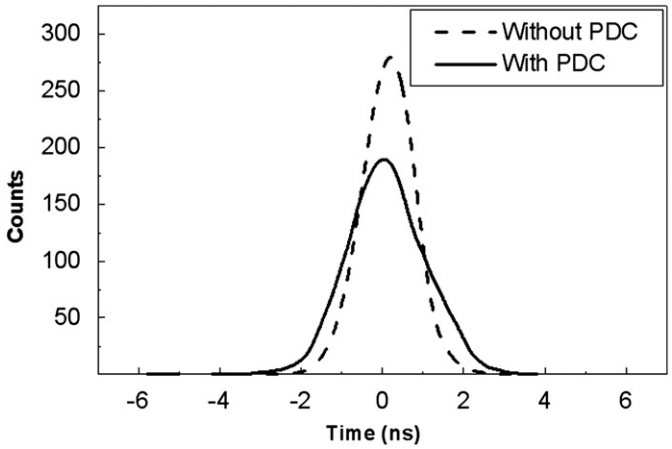

Fig. 8. Coincidence timing spectra measured with and without the position decoder circuit.

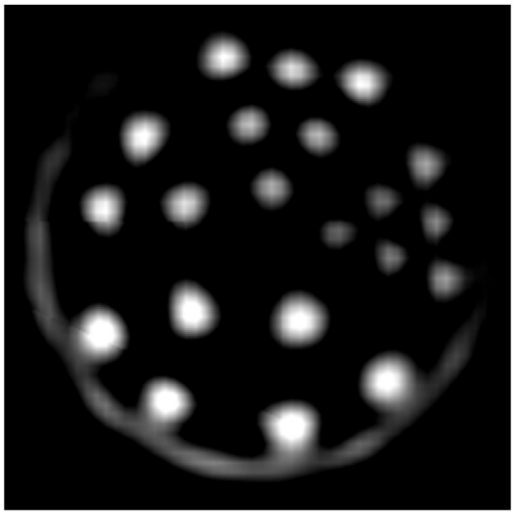

Fig. 9. Tomographic image of the hot-rod phantom acquired using proof-of-principle PET with the position decoder circuit.

interacted channel from numerous outputs of PET detectors consisting of GAPD arrays, was developed. Although the number of readout channels was reduced by a factor of 32 in the PDC developed for this study, multiplexed channel number could be readily extended using the proposed design scheme, as illustrated in Fig. 4.

Two steps were sequentially performed for identification of a valid channel among numerous inputs transferred to the PDC. In the first step, discrimination of noise or low energy scattered signals from all channel signals was performed using LLD. For global application of the threshold value for all channels of the PDC, offset levels of signals transferred to the PDC must be uniform, because if offset levels are different, the same energy threshold cannot be applied for all signals. Offset levels of each GAPD array used in this study showed little difference. Therefore, as shown in Fig. 1, an offset level translation circuit capable of independent adjustment of the offset level for each GPAD PET detector was designed.

In previous studies [8–10], the method for finding the signal with maximum amplitude was used to select a valid signal among signals with amplitude over the LLD threshold. The fastest signal identification method was applied in this study, because the analog circuit can be designed with more simplicity, and because the fastest signal corresponds to the biggest signal, which has a high probability of being a valid signal.

Gain of each channel in a multi-channel photosensor was commonly non-uniform. For example, the gain variation of a multi-anode type photomultiplier tube was typically 3:1 [13,14]. For global application of energy threshold in the multi-channel detector, the gain of all channels must be homogeneous. In this study, because the maximum gain variation of the GAPD was 1.8:1, the variable gain adjust circuit, which adjusts the gain in a range from 1 to 2, was designed to achieve gain uniformity of the PET detector, as shown in Fig. 7(b). Using the gain adjust circuit, gain uniformity was improved by 80% after gain correction.

Because the PDC needs enough time to output a GAPD signal of 250 ns width without signal loss, GAPD outputs were held for 35 ns by a signal delay circuit within the PDC. As shown in Fig. 6(b), total propagation delay time, including signal holding time, was 45 ns in the developed PDC

The difference of energy resolutions measured with and without the PDC was negligibly small. However, because output analog signal of the PDC was slightly larger than input signal and because the gain of the GAPD channel shown in Fig. 7(a) was adjusted to achieve gain homogeneity, photopeak position was increased by 5.9% using the PDC.

The coincidence timing resolution was decreased from 1.5 to 2.2 ns using the PDC because the signal transmission line length according to the location of the input channel on the printed circuit board was different. Currently, design optimization of the PDC was under investigation to decrease the time difference according to input channel. However, the measured timing resolution was comparable to that of commercial small animal

PET (<2 ns) [15,16] and human PET (<6 ns) [17], except for time-of-flight PET.

A hot-rod phantom image was successfully acquired using proof-of-principle PET with the PDC. This result demonstrated that the proposed fastest signal identification method was useful for valid channel identification and was feasible for acquisition of high quality PET using the PDC employed with the proposed method.

5. Conclusion

In this study, channel reduction techniques that employ the fastest signal identification method and the LLD method were proposed, and an analog circuit for application with these methods was fabricated. Experimental results indicate that the PDC developed for this study is not only useful for reduction of channel number of the PET detector consisting of GAPD arrays with a large number of channels, but also for PET signal processing and PET imaging. The PDC developed for this study will be extended to 36 for a human brain PET system consisting of 72 detector modules.

Acknowledgments

This study was supported in part by the Technology Innovation Program (no. 10030029) funded by the Ministry of Knowledge Economy and by the Converging Research Center Program (no. 2009-0081935) through the National Research Foundation of Korea (NRF) funded by the Ministry of Education, Science and Technology, Republic of Korea.

References

[1] A.N. Otte, J. Barral, B. Dolgoshein, J. Hose, S. Klemin, E. Lorenz, et al., Nucl. Instr. and Meth. A 545 (2005) 705.
[2] P. Buzhan, B. Dolgoshein, E. Garutti, M. Groll, A. Karakash, V. Kaplin, et al., Nucl. Instr. and Meth. A 567 (2006) 353.
[3] D.J. Herbert, V. Saveliev, N. Belcari, N.D. Ascenzo, A. Del Guerra, A. Golovin, IEEE Trans. Nucl. Sci. NS-53 (2006) 389.
[4] M. McClish, P. Dokhale, J. Christian, C. Stapels, K.S. Shah, Nucl. Instr. and Meth. A 572 (2007) 1065.
[5] S. Siegel, R.W. Silverman, Y.P. Shao, S.R. Cherry, IEEE Trans. Nucl. Sci. NS-43 (1996) 1634.
[6] R.L. Clancy, C.J. Thompsoni, J.L. Robart, A.M. Bergmad, IEEE Trans. Nucl. Sci. NS-44 (1997) 494.
[7] V. Popov, S. Majewski, B.L. Welch, Nucl. Instr. and Meth. A 567 (2006) 319.
[8] J.H. Kim, Y. Choi, K.S. Joo, B.S. Sihn, J.W. Chong, S.E. Kim, et al., Phys. Med. Biol. 45 (2000) 3481.
[9] W.W. Moses, E. Beuville, M.H. Ho, IEEE Trans. Nucl. Sci. NS-43 (1996) 1615.
[10] Y. Wu, C. Catana, S.R. Cherry, IEEE Trans. Nucl. Sci. NS-55 (2008) 463.
[11] E. Albuquerque, V. Bexiga, R. Bugalho, B. Carrico, C.S. Ferreira, M. Ferreira, et al., Nucl. Instr. and Meth. A 598 (2009) 802.
[12] M. Streun, G. Brandenburg, H. Larue, E. Zimmermann, K. Ziemons, H. Halling, Nucl. Instr. and Meth. A 486 (2002) 18.
[13] Y. Shao, S.R. Cherry, S. Siegel, R.W. Silverman, S. Majewski, Nucl. Instr. and Meth. A 390 (1997) 209.
[14] M. Streun, D. Christ, A. Hollendung, H. Larue, K. Ziemons, H. Halling, Nucl. Instr. and Meth. A 537 (2005) 402.
[15] Y.C. Tai, A. Chatziioannou, S. Siegel, J. Young, D. Newport, R.N. Goble, R.E. Nutt., S.R. Cherry, Phys. Med. Biol. 46 (2001) 1845.
[16] K. Ziemons, E. Auffray, R. Barbier, G. Brandenburg, P. Bruyndonckx, Y. Choi, et al., Nucl. Instr. and Meth. A 537 (2005) 307.
[17] J.L. Humm, A. Rosenfeld, A. Del Guerra, Eur. J. Nucl. Med. Mol. Imaging 30 (2003) 1574.